

## Charge Density Waves in Graphite: Towards the Magnetic Ultraquantum Limit

F. Arnold,<sup>1,\*</sup> A. Isidori,<sup>1,†</sup> E. Kampert,<sup>2</sup> B. Yager,<sup>1</sup> M. Eschrig,<sup>1</sup> and J. Saunders<sup>1</sup>

<sup>1</sup>Royal Holloway, University of London, TW20 0EX Egham, United Kingdom

<sup>2</sup>Hochfeld-Magnetlabor Dresden (HLD), Helmholtz-Zentrum Dresden-Rossendorf, D-01328 Dresden, Germany

(Received 21 July 2016; revised manuscript received 2 March 2017; published 26 September 2017)

Graphite is a model system for the study of three-dimensional electrons and holes in the magnetic quantum limit, in which the charges are confined to the lowest Landau levels. We report magneto-transport measurements in pulsed magnetic fields up to 60 T, which resolve the collapse of two charge density wave states in two, electron and hole, Landau levels at 52.3 and 54.2 T, respectively. We report evidence for a commensurate charge density wave at 47.1 T in the electron Landau level, and discuss the likely nature of the density wave instabilities over the full field range. The theoretical modeling of our results predicts that the ultraquantum limit is entered above 73.5 T. This state is an insulator, and we discuss its correspondence to the “metallic” state reported earlier. We propose that this (interaction-induced) insulating phase supports surface states that carry no charge or spin within the planes, but does, however, support charge transport out of plane.

DOI: 10.1103/PhysRevLett.119.136601

Semimetals like graphite and bismuth are the subject of renewed interest due to their close relation to the topological Dirac and Weyl semimetals [1–3]. Their low charge carrier density and effective mass reduce the magnetic field necessary to drive these systems into their magnetic quantum limit, in which the electronic structure is described by only a few Landau levels (LLs). In such materials this limit can be realized in state-of-the-art high-magnetic field laboratories, whereas it is inaccessible in conventional metals. The magnetic field induces a crossover from 3D to 1D physics, and the perfect nesting characteristic of 1D electron systems leads to the possibility of field-induced spin- and charge-density wave instabilities (SDWs and CDWs, respectively) with ordering wave vector along the field direction [4–7]. In the ultraquantum regime these systems are potentially subject to a rich variety of magnetic field driven topological quantum states such as the fractional quantum Hall effect and the recently discussed axial and chiral anomaly [7–11,13,14]. The clarification of the nature of the density wave instabilities in graphite, and the nature of the quantum state at high magnetic fields, is the focus of the work reported here.

Graphite is a 3D semimetal consisting of an infinite stack of graphene sheets [15,16]. The zero-field band structure is well described by the tight-binding Slonczewski-Weiss-McClure model [17–20]. The Fermi surface consists of strongly anisotropic, trigonally warped ellipsoidal electron and hole pockets located along the  $H$ - $K$ - $H$  and  $H'$ - $K'$ - $H'$  edges of the hexagonal Brillouin zone (see Fig. 1). In magnetic fields applied perpendicular to the graphene layers, the lowest-energy band ( $E_3$ , slightly hybridizing with two higher-energy bands  $E_1$  and  $E_2$  near the  $H$  points) gives rise to two 1D LLs with index  $n = -1$  and  $n = 0$ . Each LL is spin split by the Zeeman energy and has a

residual twofold valley degeneracy associated with the two inequivalent  $H$ - $K$ - $H$  and  $H'$ - $K'$ - $H'$  edges of the Brillouin zone. For magnetic fields above 8 T these are the only LLs that cross the Fermi energy. The system becomes quasi-1D, due to  $c$ -axis dispersion.

This quantum limit has been extensively investigated by magnetotransport measurements. Studies on Kish graphite showed a pronounced resistance anomaly above 22 T [21,22]. Yoshioka and Fukuyama [23] attributed the observed anomaly to the formation of a CDW in one of the lower LLs [24], and developed a mean-field theory describing the magnetic field dependence of its critical temperature. Improved LL calculations by Takada and Goto [25] showed that electron correlations play a crucial role in renormalizing the Slonczewski-Weiss-McClure LL structure. Subsequent experiments to higher fields [26,27] identified a transition at 52 T corresponding to the collapse of a density wave phase as the  $(0, \uparrow)$  or  $(-1, \downarrow)$  LL emptied. So far attempts to directly measure the gap of this putative density wave spectroscopically [28,29] have been unsuccessful.

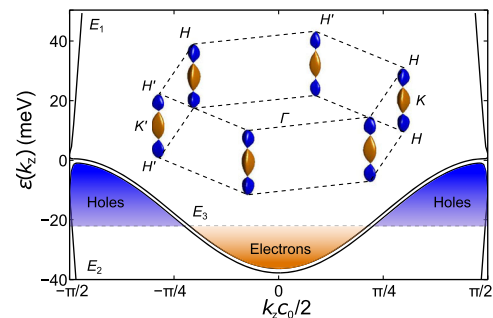


FIG. 1. Zero-field  $k_z$  dependence of graphite’s band structure along the  $H$ - $K$ - $H$  and  $H'$ - $K'$ - $H'$  edges of the Brillouin zone.

Recently, Fauqué *et al.* [12] discovered the onset of a second density-wave anomaly above 53 T, by out-of-plane transport measurements on Kish graphite up to 80 T. This state was found to collapse at 75 T into a state with metallic  $c$ -axis conductivity. These authors argued that only one of the  $(0, \uparrow)$  or  $(-1, \downarrow)$  LLs depopulates at 53 T, and, furthermore, that the  $(0, \downarrow)$  and  $(-1, \uparrow)$  levels remain populated above 75 T. On the other hand, the observation of a vanishing Hall coefficient at 53 T [30] was interpreted in terms of the depopulation of both the  $(0, \uparrow)$  and  $(-1, \downarrow)$  LLs at 53 T, as predicted theoretically [25]. It was suggested that an excitonic phase forms in the remaining  $(0, \downarrow)$  and  $(-1, \uparrow)$  levels above 53 T. Elsewhere it has been argued that an excitonic insulator phase appears at 46 T [31]. A resistance hysteresis was observed around 53 T [32]. In addition, a small feature of unclear origin (we will clarify its origin in the present work) around 47 T was reported [33]. It is clear that the evolution of the LLs with magnetic field, and their associated density wave instabilities, through the quantum limit and into the ultra-quantum limit at highest fields, remain open questions.

In this Letter we present new magnetotransport measurements on single crystal graphite, of significantly higher quality than hitherto, in conjunction with new theoretical calculations of the LL band structure, and density wave instabilities. We show that the field-induced density wave below 54.2 T, contrary to previous reports, is a superposition state of a number of incommensurate collinear CDWs with different onset and vanishing fields. One of these undergoes a lock-in transition at 47.1 T before two of the CDWs vanish due to the emptying of their corresponding LLs at 52.3 and 54.2 T, respectively. Within our model we predict that the system stays gapped at low temperatures above 54.2 T, due to additional CDWs which empty ultimately at 73.5 T. This upper threshold field defines the ultraquantum limit, above which our model predicts a LL structure such that the bulk is an insulator. This corresponds to the new phase, with observed onset at 75 T, discovered in Ref. [12]. Given the observation of the

metallic  $c$ -axis response in that phase [12], we propose that it supports a set of surface states which allow for charge transport perpendicular to the planes, although within the planes the charge and spin currents cancel. We find that interactions are crucial for this state to be insulating; without taking into account interactions the system would be metallic at these magnetic fields.

Our electrical transport measurements were performed on a single crystal of Tanzanian natural graphite [34], the quality of which significantly exceeds the commonly used Kish graphite, highly oriented pyrolytic graphite, or other natural graphites, as evidenced by de Haas–van Alphen measurements [35]. This sample quality is crucial in revealing the new features we observe; the self-doping of graphite by structural defects is minimized, reducing electron-hole charge imbalance. Our studies of the in-plane and out-of-plane magnetotransport were made in pulsed magnetic fields up to 60 T [35,36].

Figure 2 shows the in-plane resistance of the graphite crystal for fields up to 60 T and temperatures below 10 K. The in-plane resistance first increases steeply, superimposed by Shubnikov–de Haas oscillations, and saturates above 15 T due to the presence of a closed Fermi surface [7,22,50,51]. At lowest temperatures a step is observed in the in-plane resistance at around 30 T, followed by a steep increase of the resistance, reaching its maximum value at 48 T before it drops down to below its initial value at around 53 T. This behavior has already been reported for Kish and highly oriented pyrolytic graphite, and has been attributed to the formation of a DW state [12,22,27,33,52]. Similar features can also be identified in the out-of-plane transport [12,35].

In order to highlight the signatures of the transitions in our sample, the magnetic field derivatives of the in-plane magnetoresistance were calculated (see Fig. 2). Here the transitions appear as maxima and minima. We denote the observed maxima as  $\alpha$ ,  $\beta$ , and  $\gamma$ , in ascending order of their transition fields, and the corresponding minima as  $\alpha'$  and  $\beta'$ . The resolution of the two features  $\alpha'$  and  $\beta'$  is the first

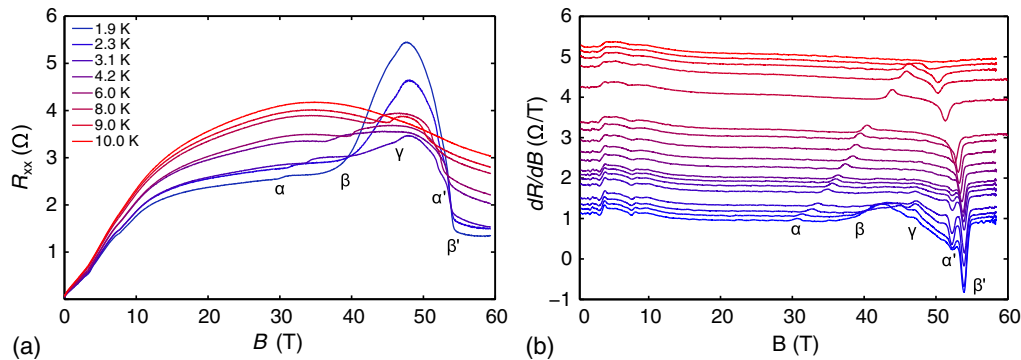


FIG. 2. (a) Magnetic field dependence of the in-plane resistance of graphite for temperatures below 10 K measured in a 25 ms 60 T pulsed field magnet. (b) Magnetic field derivatives of the in-plane resistance: The data have been offset proportional to the temperature by  $0.5 \text{ } \Omega/\text{TK}$  for clarity.  $\alpha$  and  $\beta$  denote the onset transitions of the DWs in the  $(0, \uparrow)$  and  $(-1, \downarrow)$ , whereas  $\alpha'$  and  $\beta'$  mark the field at which they vanish. At  $\gamma$  the CDW associated with the  $(0, \uparrow)$  LL undergoes a lock-in transition.

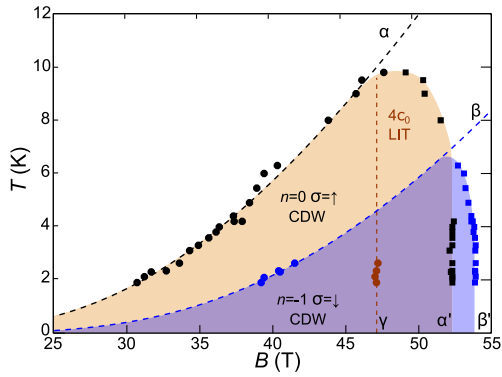


FIG. 3. Phase diagram of the CDWs in the  $(0, \uparrow)$  and  $(-1, \downarrow)$  LLs. Circles and squares are phase transitions with positive and negative differential magnetoresistance, where black represents the  $\alpha$ , blue the  $\beta$ , and other the  $\gamma$  transition. At low fields the critical temperature of  $\alpha$  and  $\beta$  increases exponentially following [23] (black and blue dashed lines):  $T_c(B) = T^* \exp\{-B^*/B\}$ , with  $T_\alpha^* = 230$  K,  $B_\alpha^* = 148$  T,  $T_\beta^* = 300$  K,  $B_\beta^* = 195$  T.

key new observation, and we also observe it in the out-of-plane transport [35]. The  $\beta'$  transition develops below 6 K alongside the  $\alpha'$  transition. In addition, we identify a new weaker feature, labeled  $\gamma$ , at  $47.1 \pm 0.1$  T, which is resolved below 3 K and represents the onset of another resistance increase. The temperature dependence of these transitions is shown in Fig. 3 [35].

We now discuss the theoretical interpretation of these features, based on our new numerical calculations of the LL structure including the Hartree-Fock self-energy, following the framework of Ref. [25]. In the quantum limit, the system is understood in terms of the one-dimensional dispersion of the lowest, spin-split, electron and hole LLs, and their density wave instabilities. We investigate

closely the magnetic field dependence of the putative nesting vectors in all four LLs that are close to the Fermi level (see Fig. 3). We calculate the renormalized LLs by including the electron self-energy in a fully self-consistent manner [35]. The effect of short-range correlations, neglected by the conventional random-phase approximation, is included via the Hubbard local-field correction [37,38] to the effective electron-electron interaction. The inclusion of this correction is crucial in order to get a quantitative agreement between the theoretical LL structure and the experimental data. We use the experimental value of  $B_\alpha$  to fix the tuning parameter that characterizes our theory [35], namely, the static relative permittivity.

We find that the sharpest new features at  $B_\alpha = 52.3 \pm 0.1$  and  $B_{\beta'} = 54.2 \pm 0.1$  T correspond to two distinct first-order transitions (see Figs. 3 and 4) associated with the abrupt depopulation of both the  $(0, \uparrow)$  (electronlike) and  $(-1, \downarrow)$  (holelike) LLs. We argue below that the splitting of the transitions arises from the breaking of valley degeneracy. The first-order character of the  $\alpha'$  and  $\beta'$  transitions, predicted by our theory, is experimentally confirmed by the clear evidence of hysteresis in both, as shown in Fig. 4(c).

Furthermore, our calculations show that at  $B_\gamma = 48$  and  $B_e = 68$  T, the nesting vectors of the intraband CDWs, i.e.,  $Q^{(0,\uparrow)}$  and  $Q^{(-1,\downarrow)}$  as well as  $Q^{(0,\downarrow)}$  and  $Q^{(-1,\uparrow)}$  [Fig. 4(b)] take the values of  $2\pi/4c_0$  and  $2\pi/3c_0$ , respectively, corresponding to commensurate wavelengths of  $4c_0$  and  $3c_0$  (the lattice parameter  $c_0$  is twice the distance between adjacent graphene layers). This suggests the  $\gamma$  feature, observed experimentally around 47.1 T and temperatures below 3 K (see Fig. 2) is a lock-in transition of the corresponding CDW from an incommensurate state to a “phase-locked” commensurate order [35,39–45,53].

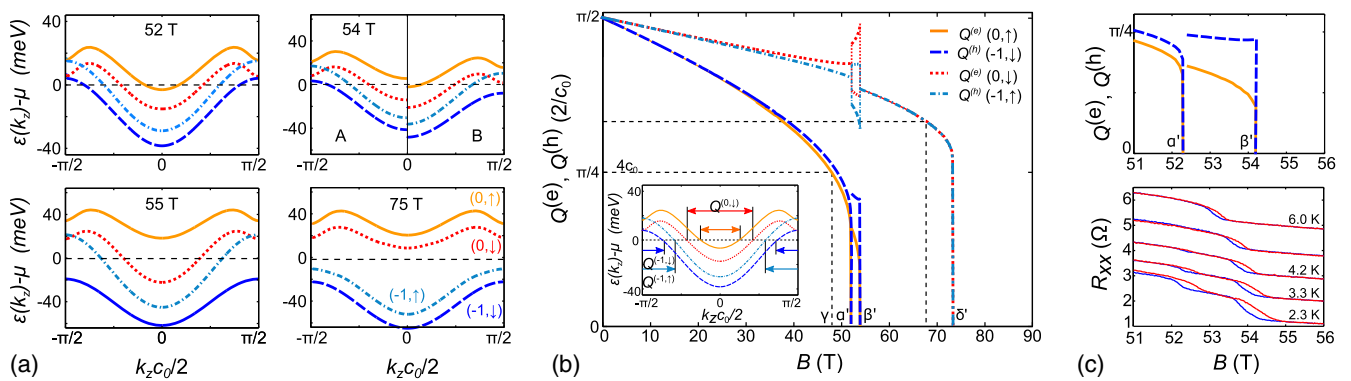


FIG. 4. (a) Renormalized LL structure in the ultraquantum limit: Above 8 T only four LLs cross the Fermi energy. At 54 T valley degeneracy is lifted leading to two differentially doped sets of LLs, here A and B refer to the  $H$ - $K$ - $H$  and  $H'$ - $K'$ - $H'$  valleys. (b) CDW nesting vectors  $Q$  up to 90 T. Holelike levels have nesting vectors given by  $Q^{(h)} = 2k_F^{(h)} = 2\pi/c_0 - 2k_F$  (see inset). All  $Q$ s decrease with increasing magnetic field due to the upward and downward shift of the electronlike  $(0, \sigma)$  and holelike  $(-1, \sigma)$  LLs, before vanishing in a first-order transition at  $B_\alpha = 52.3$ ,  $B_{\beta'} = 54.2$ , and  $B_\gamma = 73.5$  T. The nesting vector of the  $(0, \uparrow)$  LL becomes commensurate at  $B_\gamma = 48$  T. (c) Close-up of the nesting vectors in the vicinity of the first-order  $\alpha'$  and  $\beta'$  transitions (top panel) and observed resistance hysteresis (bottom panel): The red curves show the magnetic field up sweeps, whereas blue curves correspond to the down sweeps.

Lock-in transitions are characteristic fingerprints of CDW systems [54], where translational invariance of the charge modulation is lost with respect to the lattice [35].

We now elaborate on the splitting of the  $\alpha'$  and  $\beta'$  transitions. In the simplest calculation these transitions occur at the same field value, in an undoped sample [55]. To account for the splitting, while preserving overall charge balance, we need to either lift the valley degeneracy or invoke an inhomogeneous state with spatial phase separation. In the first scenario, a spontaneous breaking of the valley degeneracy leads to a splitting between the LLs originating from the Fermi surface pockets located along the two inequivalent  $H$ - $K$ - $H$  and  $H'$ - $K'$ - $H'$  edges of the Brillouin zone (see Fig. 1) similar to what has been observed in bismuth [14]. The system is then characterized by two inequivalent sets of LLs, one for each valley, allowing each set of LLs to develop a finite, equal and opposite, charge imbalance in the narrow region between  $B_{\alpha'}$  and  $B_{\beta'}$ . In this magnetic-field region both valleys are characterized by three populated and one empty LL; the empty level in the hole-doped valley is the electronlike  $(0, \uparrow)$  LL, whereas in the electron-doped valley the empty level is the holelike  $(-1, \downarrow)$  (see Fig. 4). Since the two valleys are now characterized by inequivalent nesting vectors, the collinear CDW order observed below  $\alpha'$  turns into a valley density-wave state, with an additional commensurate in-plane modulation originating from the reciprocal lattice vectors connecting the two valleys. We find that such a state is promoted by moving the system towards another lock-in state [35].

To account quantitatively for the observed splitting between  $\alpha'$  and  $\beta'$  we predict a charge imbalance, parameterizing the broken valley degeneracy of  $(p - n)/(p + n) = \pm 0.128$  in the two valleys, where  $p$  ( $n$ ) denotes the hole (electron) carrier density. The opposite imbalance in the two valleys guarantees the overall charge balance of the system.

We now turn to the ultraquantum limit. We first note that, for magnetic fields above  $\beta'$ , the populated levels are  $(0, \downarrow)$  (electronlike) and  $(-1, \uparrow)$  (holelike). These LLs are still characterized by finite nesting vectors. Note that the nesting vectors arising from these bands are identical due to the charge balance between electron and hole carriers.

Our calculations show that both levels become depopulated at 73.5 T (see Fig. 4). This state was first theoretically identified by Ref. [25] in a computation at 200 T. Our predicted numerical value of  $B_{\beta'}$  is in remarkable agreement with the measured critical field of 75 T for the reentrant transition of the upper density-wave phase observed in Ref. [12]. Furthermore, we predict that the nesting vectors of a putative CDW in the  $(0, \downarrow)$ ,  $(-1, \uparrow)$  levels gives rise to an additional lock-in transition with a wavelength of  $3c_0$  at 68 T. Observation of this transition would conclusively identify the DW instabilities in this field range as CDWs.

Our finding that the  $(0, \downarrow)$  and  $(-1, \uparrow)$  states empty above 75 T refutes the proposed energy level scheme to account for the observed metallic conductivity in this field regime, in Ref. [12], where it is claimed that the  $(0, \downarrow)$  and

$(-1, \uparrow)$  states remain occupied. In contrast, above 75 T we find that the bulk should be fully gapped.

We speculate that low temperature transport may be expected to occur via a 2D chiral sheath of extended surface states [12,56–61]. These surface states are protected against weak impurity scattering. This leads to a ballistic in-plane transport along the edges of the sample, in the direction perpendicular to the magnetic field. Taking into account valley degeneracy, all four LLs contribute, leading to a cancellation of the charge and spin currents. Nevertheless metallic conductivity is observed in the out-of-plane direction [12], and we propose that this is accounted for by interlayer hopping occurring at the sample edges [57–59]. At magnetic fields between 55 and 75 T the Fermi energy crosses the  $(0, \downarrow)$  and  $(-1, \uparrow)$  LLs. The wave functions of surface states have finite overlap with bulk states and are scattered by bulk impurities, which renders transport via these states diffusive, yielding a thermally activated out-of-plane conductance at temperatures below the DW transition, as observed [12]. Studies of in-plane transport in this field regime should be of great interest.

From our assignment of the Landau level structure, it appears that in the ultraquantum limit graphite above 75 T is a fully gapped state in the bulk, an insulator, due to the strong electron correlations on the LL band structure. This new state potentially harbors an abundance of new physics and is experimentally accessible in state-of-the-art pulsed magnetic field facilities. There is current interest in systems where emergent band structure leads to a topologically nontrivial insulating state, topological Kondo insulators being one example [62,63]. The observation of metallic out-of-plane transport [12] opens a new playground for studying surface states in interaction-induced insulators, with the possibility of a topological phase transition at fields beyond 75 T.

In conclusion, the direct observation, in high quality samples, of the depopulation of two LLs at 52.3 and 54.2 T, and the commensuration of the DW at 48 T imposes severe constraints on the nature of the field-induced DW instabilities in graphite. We can theoretically account for these features, and correctly predict the field quenching of the DWs above 54 T, observed recently [12]. We believe that the most likely scenario at  $B < B_{\alpha'}$  and  $T = 0$  is CDWs in each of the four LLs. A full discussion of all possible nesting instabilities and DW scenarios and the logic behind this proposal is presented in Ref. [35], where the signatures from in-plane and out-of-plane transport are also discussed. A test of this hypothesis would be the observation of the lockin transition we predict at 68 T.

The authors wish to thank T. Förster, J. Wosnitza, T. Herrmansdörfer, and S. Zherlitsyn for experimental support at the Hochfeld Magnetlabor Dresden (HLD). We acknowledge the support of the HLD-HZDR, member of the European Magnetic Field Laboratory (EMFL) as well as the Hubbard Theory Consortium, the Max Planck Society

(MPRG Physics of Unconventional Metals and Superconductors, E. Hassinger) and the Engineering and Physical Science Research Council (EPSRC Grants No. EP/H048375/1 and No. EP/J010618/1).

\*Present address: Max Planck Institute for Chemical Physics of Solids, Nöthnitzer Str. 40, 01187 Dresden, Germany.

†Present address: Scuola Internazionale Superiore di Studi Avanzati (SISSA), Via Bonomea 265, 34136 Trieste, Italy.

- [1] Z. K. Liu, B. Zhou, Y. Zhang, Z. J. Wang, H. M. Weng, D. Prabhakaran, S. K. Mo, Z. X. Shen, Z. Fang, X. Dai, Z. Hussain, and Y. L. Chen, *Science* **343**, 864 (2014).
- [2] M. Neupane, S. Y. Xu, R. Sankar, N. Alidoust, G. Bian, C. Liu, I. Belopolski, T. R. Chang, H. T. Jeng, H. Lin, A. Bansil, F. Chou, and M. Z. Hassan, *Nat. Commun.* **5**, 3786 (2014).
- [3] H. Weng, C. Fang, Z. Fang, B. A. Bernevig, and X. Dai, *Phys. Rev. X* **5**, 011029 (2015).
- [4] A. W. Overhauser, *Phys. Rev. Lett.* **4**, 462 (1960).
- [5] A. W. Overhauser, *Phys. Rev.* **167**, 691 (1968).
- [6] V. Celli and N. D. Mermin, *Phys. Rev.* **140**, A839 (1965).
- [7] B. I. Halperin, *Jpn. J. Appl. Phys.* **26**, 1913 (1987).
- [8] K. Behnia, L. Balicas, and Y. Kopelevich, *Science* **317**, 1729 (2007).
- [9] A. Banerjee, B. Fauqué, K. Izawa, A. Miyake, I. Sheikin, J. Flouquet, B. Lenoir, and K. Behnia, *Phys. Rev. B* **78**, 161103(R) (2008).
- [10] H. Yang, B. Fauqué, L. Malone, A. B. Antunes, Z. Zhu, C. Uher, and K. Behnia, *Nat. Commun.* **1**, 47 (2010).
- [11] J. Alicea, Unexpected richness in the high-field physics of graphite, Comment on Ref. [12] published in the Journal Club for Condensed Matter Physics JCCM-AUGUST-2014-01.
- [12] B. Fauqué, D. LeBoeuf, B. Vignolle, M. Nardone, C. Proust, and K. Behnia, *Phys. Rev. Lett.* **110**, 266601 (2013).
- [13] H. B. Nielsen and M. Ninomiya, *Phys. Lett. B* **130**, 389 (1983).
- [14] R. Kuechler, L. Steinke, R. Daou, M. Brando, K. Behnia, and F. Steglich, *Nat. Mater.* **13**, 461 (2014).
- [15] K. S. Novoselov, A. K. Geim, S. V. Morozov, D. Jiang, M. I. Katsnelson, I. V. Grigorieva, S. V. Dubonos, and A. A. Firsov, *Nature (London)* **438**, 197 (2005).
- [16] A. H. C. Neto, F. Guinea, N. M. R. Peres, K. S. Novoselov, and A. K. Geim, *Rev. Mod. Phys.* **81**, 109 (2009).
- [17] P. R. Wallace, *Phys. Rev.* **71**, 622 (1947).
- [18] J. W. McClure, *Phys. Rev.* **108**, 612 (1957).
- [19] J. C. Slonczewski and P. R. Weiss, *Phys. Rev.* **109**, 272 (1958).
- [20] J. W. McClure, *Phys. Rev.* **119**, 606 (1960).
- [21] S. Tanuma, R. Inada, A. Furukawa, O. Takahashi, Y. Iye, and Y. Onuki, *Physics in High Magnetic Fields: Electrical Properties of Layered Materials at High Magnetic Fields*, Springer Series in Solid-State Sciences (Springer, Berlin, Heidelberg, 1981), Vol. 24, p. 316.
- [22] Y. Iye, P. M. Tedrow, G. Timp, M. Shayegan, M. S. Dresselhaus, G. Dresselhaus, A. Furukawa, and S. Tanuma, *Phys. Rev. B* **25**, 5478 (1982).
- [23] D. Yoshioka and H. Fukuyama, *J. Phys. Soc. Jpn.* **50**, 725 (1981).
- [24] K. Nakao, *J. Phys. Soc. Jpn.* **40**, 761 (1976).
- [25] Y. Takada and H. Goto, *J. Phys. Condens. Matter* **10**, 11315 (1998).
- [26] H. Yaguchi and J. Singleton, *Phys. Rev. Lett.* **81**, 5193 (1998).
- [27] H. Yaguchi and J. Singleton, *J. Phys. Condens. Matter* **21**, 344207 (2009).
- [28] Y. I. Latyshev, A. P. Orlov, D. Vignolles, W. Escoffier, and P. Monceau, *Physica (Amsterdam)* **407B**, 1885 (2012).
- [29] F. Arnold, B. Yager, E. Kamper, C. Putzke, J. Nyéki, and J. Saunders, *Rev. Sci. Instrum.* **84**, 113901 (2013).
- [30] K. Akiba, A. Miyake, H. Yaguchi, A. Matsuo, K. Kindo, and M. Tokunaga, *J. Phys. Soc. Jpn.* **84**, 054709 (2015).
- [31] Z. Zhu, R. D. McDonald, A. Shekhter, B. J. Ramshaw, K. A. Modic, F. F. Balakirev, and N. Harrison, *Sci. Rep.* **7**, 1733 (2017).
- [32] H. Yaguchi, M. Tokunaga, A. Matsuo, and K. Kindo, Exploration of the multiple field induced density wave phase in graphite using 75-t-class pulsed magnetic fields (unpublished).
- [33] H. Yaguchi, Y. Iye, T. Takamasu, and N. Miura, *Physica (Amsterdam)* **184B**, 332 (1993).
- [34] Naturally Graphite, Nanotech Innovations, Michigan Technological University, 1400 Townsend Drive, Houghton, Michigan 49931-1295, United States.
- [35] See Supplemental Material at <http://link.aps.org/supplemental/10.1103/PhysRevLett.119.136601> for further experimental and theoretical details that support the finding of multiple CDWs in graphite. A complete discussion of all possible nesting scenarios within the four lowest Landau levels is presented, which includes Refs. [18,19,22,29,31,34,36–49].
- [36] S. Zherlitsyn, T. Herrmannsdörfer, B. Wustmann, and J. Wosnitza, *IEEE Trans. Appl. Supercond.* **20**, 672 (2010).
- [37] J. Hubbard, *Proc. R. Soc. A* **243**, 336 (1958).
- [38] K. S. Singwi, M. P. Tosi, R. H. Land, and A. Sjölander, *Phys. Rev.* **176**, 589 (1968).
- [39] P. Lee, T. Rice, and P. Anderson, *Solid State Commun.* **14**, 703 (1974).
- [40] W. L. McMillan, *Phys. Rev. B* **14**, 1496 (1976).
- [41] P. Bak and V. J. Emery, *Phys. Rev. Lett.* **36**, 978 (1976).
- [42] A. D. Bruce, R. A. Cowley, and A. F. Murray, *J. Phys. C* **11**, 3591 (1978).
- [43] A. D. Bruce and R. A. Cowley, *J. Phys. C* **11**, 3609 (1978).
- [44] R. A. Cowley, *Adv. Phys.* **29**, 1 (1980).
- [45] S. Sugai, Y. Takayanagi, and N. Hayamizu, *Phys. Rev. Lett.* **96**, 137003 (2006).
- [46] F. Arnold, C. Shekhar, S. C. Wu, Y. Sun, R. D. dos Reis, N. Kumar, M. Naumann, M. O. Ajeesh, M. Schmidt, A. G. Grushin, J. H. Bardarson, M. Baenitz, D. Sokolov, H. Borrmann, M. Nicklas, C. Felser, E. Hassinger, and B. Yan, *Nat. Commun.* **7**, 11615 (2016).
- [47] A. Pippard, *Magnetoresistance in Metals* (Cambridge University Press, Cambridge, England, 1998).
- [48] R. D. Reis, M. O. Ajeesh, N. Kumar, F. Arnold, C. Shekhar, M. Naumann, M. Schmidt, M. Nicklas, and E. Hassinger, *New J. Phys.* **18**, 085006 (2016).
- [49] Y. Iye and G. Dresselhaus, *Phys. Rev. Lett.* **54**, 1182 (1985).

- [50] N. B. Brandt, G. A. Kapustin, V. G. Karavaev, A. S. Kotosonov, and E. A. Svistova, *Sov. Phys. JETP* **40**, 564 (1975).
- [51] K. Sugihara and J. A. Woollam, *J. Phys. Soc. Jpn.* **45**, 1891 (1978).
- [52] S. Uji, J. S. Brooks, and Y. Iye, *Physica (Amsterdam)* **246–247B**, 299 (1998).
- [53] D. E. Moncton, J. D. Axe, and F. J. DiSalvo, *Phys. Rev. Lett.* **34**, 734 (1975).
- [54] P. Monceau, *Charge Density Waves in Solids*, Modern Problems in Condensed Matter Science, edited by L. Gorkov and G. Grüner (North Holland, Amsterdam, 1989), Vol. 25.
- [55] A uniform charge imbalance of 0.11 is required to explain the observed splitting, which is unphysical [30].
- [56] A. H. MacDonald, *Phys. Rev. Lett.* **64**, 220 (1990).
- [57] J. T. Chalker and A. Dohmen, *Phys. Rev. Lett.* **75**, 4496 (1995).
- [58] L. Balents and M. P. A. Fisher, *Phys. Rev. Lett.* **76**, 2782 (1996).
- [59] S. Cho, L. Balents, and M. P. A. Fisher, *Phys. Rev. B* **56**, 15814 (1997).
- [60] D. P. Druist, P. J. Turley, K. D. Maranowski, E. G. Gwinn, and A. C. Gossard, *Phys. Rev. Lett.* **80**, 365 (1998).
- [61] A. F. Young, J. D. Sanchez-Yamagishi, B. Hunt, S. H. Choi, K. Watanabe, T. Taniguchi, R. C. Ashoori, and P. Jarillo-Herrero, *Nature (London)* **505**, 528 (2014).
- [62] M. Dzero, K. Sun, V. Galitski, and P. Coleman, *Phys. Rev. Lett.* **104**, 106408 (2010).
- [63] M. Dzero, J. Xia, V. Galitski, and P. Coleman, *Annu. Rev. Condens. Matter Phys.* **7**, 249 (2016).